Tight Hammering for Plastic Zone of Materials

Tight Hammering for Plastic Zone of Materials

WANG Yingwei[1], MA Zhongnan[1], DONG Xin [1], YAN Qingguang[1], GAO Jinzhu[2], GAI Xiuying[2]

[1]Jilin University, Changchun 130022, China
[2]Institute of Metals, Chinese Academy of Sciences, Shenyang 110016, China

Abstract. Considering the failure due to cracks and peeling from curved surfaces of complex components, we used the tight hammering method to study the internal plastic deformation zones of curved-surface Q235 steel specimens after hammering shock and display relevant information. A Dino-capture microscope and a ZEISS LSM 700 laser scanning microscope were used to obtain and fit the morphologic data of rebounded zones and identify effective boundary points. Data of the boundary points were processed by least squares fitting. After curved-surface specimens of different curvature radii and planar specimens were hammered by the SR5.5 punch head and the plastic zones on the tight curved surfaces were all circularly-shaped at different impact strokes. The hammer traces were symmetrical spatially, indicating the internal plastic zones of the tight curved-surface specimens were approximately spherically-shaped. Deformations of plastic zones at external corners were large in magnitude and small in area, while those at internal corners were small in magnitude and large in area.

1. Introduction

The rapid industrial development has intensified the demand for high value industrial equipment and made it urgent to improve its fatigue life and reduce its manufacturing costs by appropriate surface treatment. Component surfaces can be strengthened by shot peening, rolling, hole expansion, explosion shock and friction strengthening [1, 2]. It is because any type of surface deformation processing will induce plastic deformation on metal surfaces and finally trigger high-density dislocation that can efficiently inhibit the initiation and propagation of surface microcracks [3-5]. So far, the main research methods of plastic zone include stress relaxation [6, 7], magnetic method [8, 9], X-ray diffraction [10], and ultrasound & shock indentation [11]. These methods all have cons and pros.

In recent years, there has been more studies in this field [12-19]. Underwood measured residual stress using surface displacement around indentations [15]. Chen et al. studied plastic deformation zones using impact indentation method and finite element numerical simulation [17-19]. Maximo et al. built a 3D single-hole expansion model and verified its practicability [20]. However, the analysis of plastic zone was dependent on finite element numerical simulation, in which the process model presetting and boundary condition setting largely affected the analytical results, as the evident indirectness of result estimation increased errors. Moreover, no novel research method or influential study has been reported in recent years.

Therefore, we innovatively proposed a tight hammering method for curved-surface plastic zones and succeeded in displaying the information of plastic deformation zone in curved surfaces. Specifically, plastic zones were observed under laser scanning confocal microscopy, and together with

mathematical theoretical computation. Their shapes and areas were studied. In particular, the effects of surface morphology and other factors were analyzed.

2. Experimental Section

2.1. Experiment materials

The tested material Q235 steel was made into strip specimens 170 mm × 20 mm × 30 mm (length × width × height). The hammered surface and tight surface of each strip were ground. After that, the surface roughness was 0.4 μm and hardness was 117HBW/10/3000.

2.2. Experimental methods

Metal-based pseudo-isotropic specimens were designed. Internal plastic deformations occurred after planar or curved surfaces were vertically hammered by a spherical punch head. These deformations would leave round-pit- shaped traces on material surfaces. These traces were the exposed surfaces of internal plastic zones, which were located beneath the traces and resulted from plastic rheological change under hammering compression.

Figure 1&2 show the schematic of hammer test and the specimens after hammering. The hammer test device consisted of a manual two-dimensional platform with a movement precision of 0.05 mm in both X- and Y-directions, a bracket, a straight-line guide rail, a slider and a 4.7 kg punch head. Two specimens were tightened together by a tightening device and simulated as one specimen. The tightening force should be large enough, which ensured instantaneous opening of tight fissures would not occur during the hammering process and deformation would occur immediately after the tight fissures were hammered by the punch head. After the tightening force was withdrawn, a rebounded convex zone (short for rebounded zone) would appear on the tight surface after the two tightened specimens were separated. The platform in the middle of this convex zone was the plastic deformation zone (short for plastic zone). The measuring points were set at appropriate distance, which avoided between-point interaction. Figure 3 shows the frontal hammer traces and rebounded zone on tight surfaces of separated specimens.

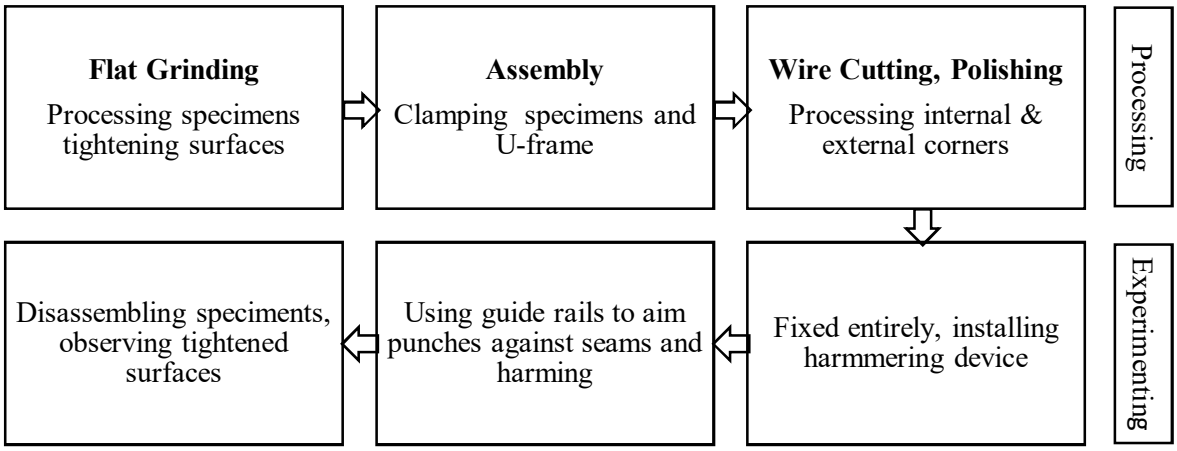

Figure 1. Schematic Illustration of Tight Hammering Method.

Considering the effects of hammering work, curved-surface shape and curvature radius on the results, we designed an SR5.5 hard alloy punch head with six impact strokes (25 mm, 50mm, 75 mm, 100 mm, 125 mm, 150 mm), internal corners and external corners of plane or curved-surfaces with five curvature radii (8 mm, 10 mm, 12 mm, 14 mm, 16 mm).

The specimens were observed and measured using a Dino-capture microscope 30×, which returned information about the surface shapes of rebounded convex zones. The rebounded convex zones were scanned using a ZEISS LSM 700 laser confocal microscope at z-axis resolution of 10 nm, and

diagonal line of 18 mm in the scanning field, which returned precise 3D data of rebounded convex zones.

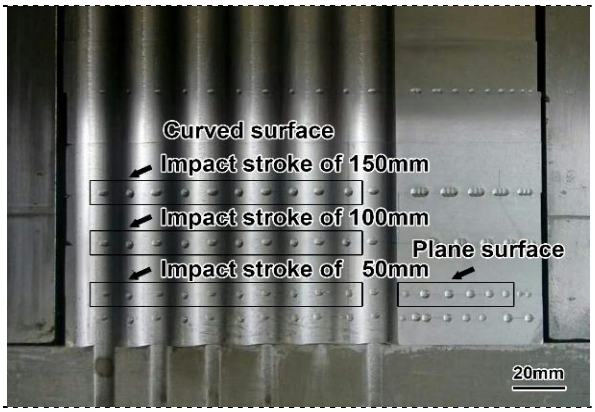

Figure 2. The Specimens after Hammering.

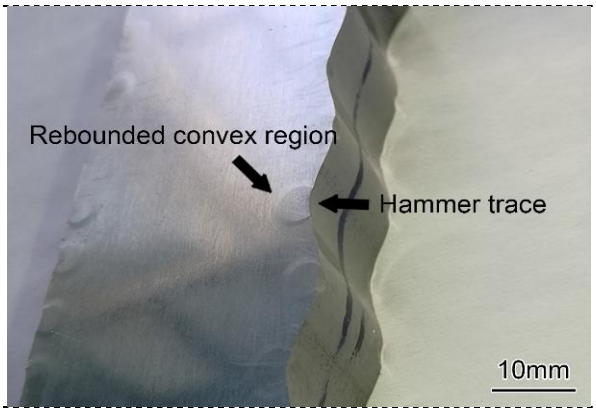

Figure 3. The Frontal Hammer Trace and the Rebounded Convex Region on the Tight Surface of Separated Sample.

2.3. Analytical methods

To accurately describe the shapes of plastic zones, we defined a plane perpendicular to the sample that divided the plastic zone into two equal parts. This plane, called the sagittal plane, had an intersecting line (called the sagittal line) with the surface of the rebounded zone. By adjusting the value of coordinate X, we could move the sagittal plane to right or left, forming a parallel sagittal plane, and the corresponding intersecting line was called the sagittal parallel line. Functions were detected using a laser confocal scanning microscope, which produced the 3D coordinates of 40 equidistant sagittal parallels passing through the rebounded convex zone. The 40 lines were fitted separately by Logistics [21]. The statistic R^2=0.957 (with the sagittal parallel line at X=3.677 as example) indicates the fitting effect is good and this model is ideal for determination of real morphology (1):

$$Z = h_2 + \frac{h_1 - h_2}{1 + \left(\frac{Y}{Y_0}\right)^p} \quad (1)$$

Where Z is the rebounded height; Y is the y-axis coordinate; h_2 is height of undeformed zone; h_1 is the height of plastic zone; Y_0 is the position of largest deformation; p is the slope of turning point.

The fitted curves were processed by 3-order derivation against y, which resulted in zero-point Y_1 and Y_2 [22], where Y_2 is an effective boundary point of the rebounded zone. In this way, the effective boundary points of all sagittal parallel lines were determined.

Least squares fitting [23] of these points produced a fitted circular curve. The accuracy of the fitting results was estimated via χ^2 test to be χ^2=48.88<$\chi^2_{0.05}(37)$ [24], indicating the boundaries of the plastic zone were circular- shaped.

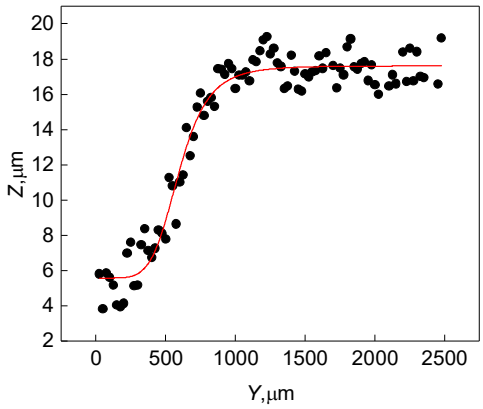

Figure 4. Sagittal Parallel Scatter Diagram Fitting of X=3.677.

Figure 4 shows the schematic diagram of fitting results in the xOy coordinate system. The projected area of the plastic zone (A_P) is the area enclosed by minor arc AB and major arc ACB. A_P in the plastic zone from the SR5.5 spherical punch head is 12.26 mm^2 at the impact stroke of 150 mm; the largest height H of hammered plastic zone is 3.92 mm, while the residual stress field depth formed by shot peening is less than 0.5 mm [25]. It is indicated the hammering method can produce a plastic zone deeper than that formed by shot peening surface strengthening, and ensures the precision-machined parts reserve a prepressing stress layer with appropriate depth, which contributes to prolonging the fatigue life of precision-machined parts.

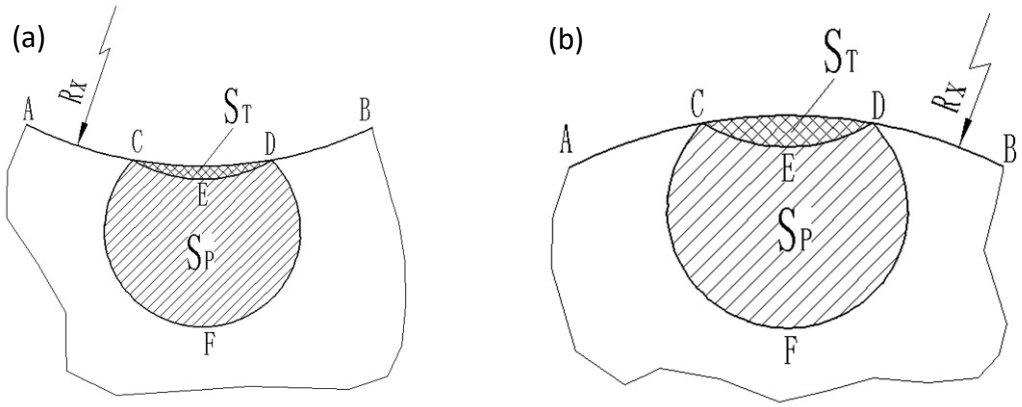

Figure 5. Projected Schematic Illustration of the Hammering Traces and the Plastic Zone at the Internal and External Corner.

3. Results and discussion

3.1. Results

Figures 6-8 show the rebounded convex zones generated with the SR5.5 punch head, internal corner with curvature radius R=10 mm, external corner with R=12 mm and impact strokes of 50 mm, 100 mm and 150 mm, respectively. The platform is clearly raised at the hampered place on the tight surface and surrounded by a ring-shaped transition zone, which is surrounded by the undeformed or original morphology. The rebounded zone appeared because the tightening force on the tight surface after hammering was large enough to inhibit the rebounding of the plastic rheological zone, and after the samples were separated, the withdrawal of the tightening force released the pressure stress, so the plastic zone rebounded and raised, forming a rebounded convex zone, which brought up the metals around the plastic zone, forming a transition zone.

Figure 12-14(a) shows the plastic zone laser confocal images and fitting results with the SR5.5 punch head at impact stroke of 150 mm, on plane; internal corner at impact stroke of 50 mm, curvature radius R =10 mm; external corner with impact stroke of 50 mm, R=12 mm. Clearly, plastic zones in these three situations are all circular-shaped, the position closer to the hammering place is redder, and the rebounded height after hammering is larger.

Figure 12-14(b) show the rebounded convex zones of three different shapes at different impact strokes and the fitting results of effective boundary points on sagittal parallel lines. As data of statistic χ^2 are all smaller than $\chi^2_{0.05}(37)$ in the table 1, which verifies the plastic zone boundaries are circular-shaped. Table 1 shows the fitting and calculated results of plastic zones with internal corner R=10 mm and external corner R=12 mm on different impact strokes.

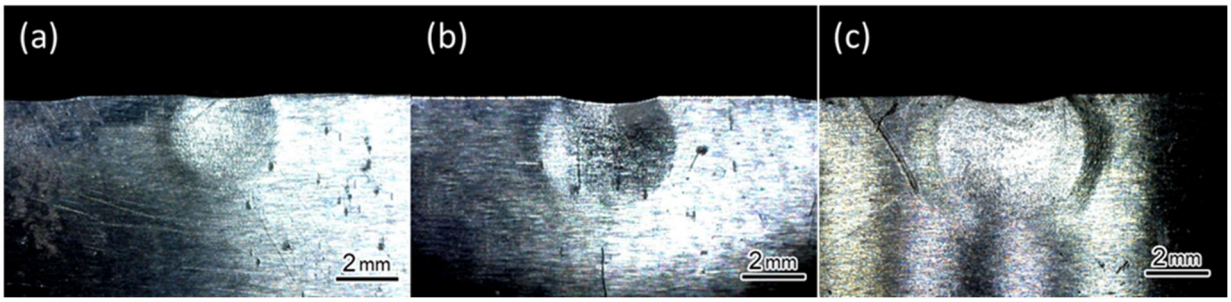

Figure 6. The Rebounded Convex Region of Impact Strokes of (a) 50 mm, (b) 100 mm and (c) 150 mm.

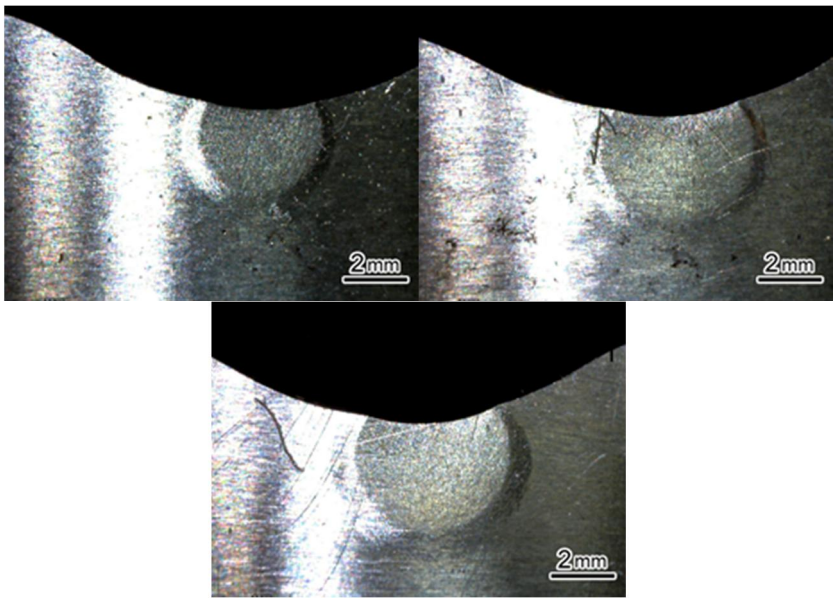

Figure 7. Rebounded Convex Region of Impact Strokes of (a) 50 mm, (b) 100 mm and (c) 150 mm of Curvature Radius R= 10 mm of Internal Corner.

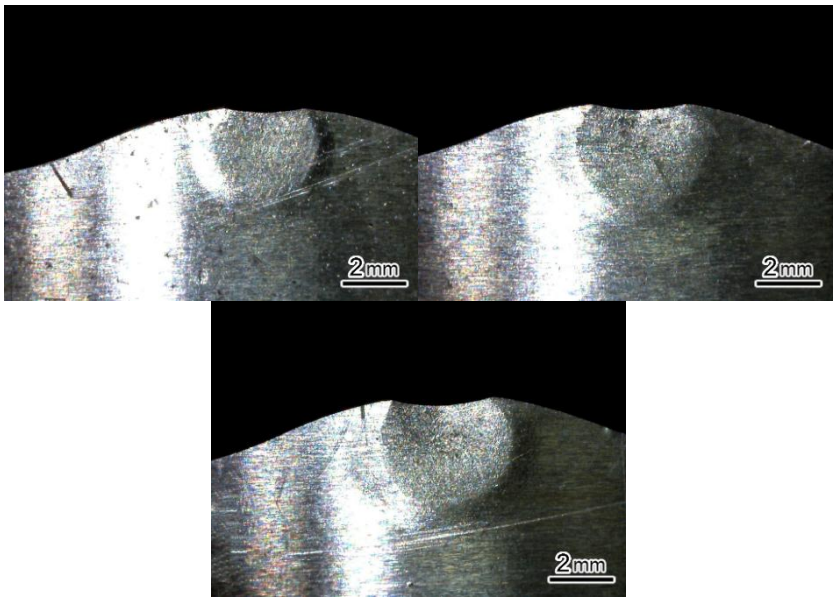

Figure 8. Rebounded Convex Region of Impact Strokes of (a) 50 mm, (b) 100 mm and (c) 150 mm of Curvature Radius R= 12mm of External Corner.

Table 1. Plastic Zone Fitting and Calculation Results of SR5.5 punch Head under Different Impact Strokes.

R_C / (mm)	*L* / mm	*R* / mm	*H* / mm	A_P/mm^2	χ^2
Pl	150	2.26	3.92	12.26	48.88
In10	50	1.87	3.41	10.52	47.64
Ex12	50	1.55	2.83	7.23	50.33

Note: R_C—curvature radius, *Pl*—plane, *In*—internal corners, *Ex*—external corners, *L*—impact stroke, *R*—radius, *H*—depth, A_P—area of plastic zone, χ^2—statistic

3.2. *Discussion*

The corresponding data were calculated using the method in Section 2.3. Figure 9 shows the changing trend of plastic zone area at impact strokes are 50 mm, 100 mm, 150 mm, internal corner (In) and external corner (Ex) with curvature radius of 8 mm, 10 mm, 12 mm, 14 mm, 16 mm. Clearly, as the curvature radius rises, the plastic zone area does not change significantly. For the same surface shape, the plastic zone area increases with the rise of impact stroke. For the same impact stroke, the plastic zone area formed at the internal corner is far larger than that at the external corner. Figure 10 shows the change trend of plastic zone area of plane (Pl), internal corner (In) and external corner (Ex) at impact strokes of 50 mm, 100 mm and 150 mm. It is indicated that the plastic zone areas are enlarged with the rise of impact stroke, and the areas at internal corners are bigger than those at internal corners and flat plane. Those plastic areas on the plane were changed rapidly with the increase of impact stroke, but those at the internal external corners were changed slowly. This is because the plastic strain energy of hammering affects the deformation degree and scope of the plastic zone, which are reflected by the rebounded height and plastic zone area, respectively. We divided the area value of the hammered pits from corresponded plastic zones, in order to describe the size relationship between them. The data thus calculated is called deformation degree (α). The plastic zone deformation at the external corner is large in degree and small in scope, but that at the internal corner is small in degree and large in scope.The deformation degree of the internal corner gradually enlarged with the increase of the radius of curvature, while the deformation degree of the external corner is on the contrary, as shown in figure 11.

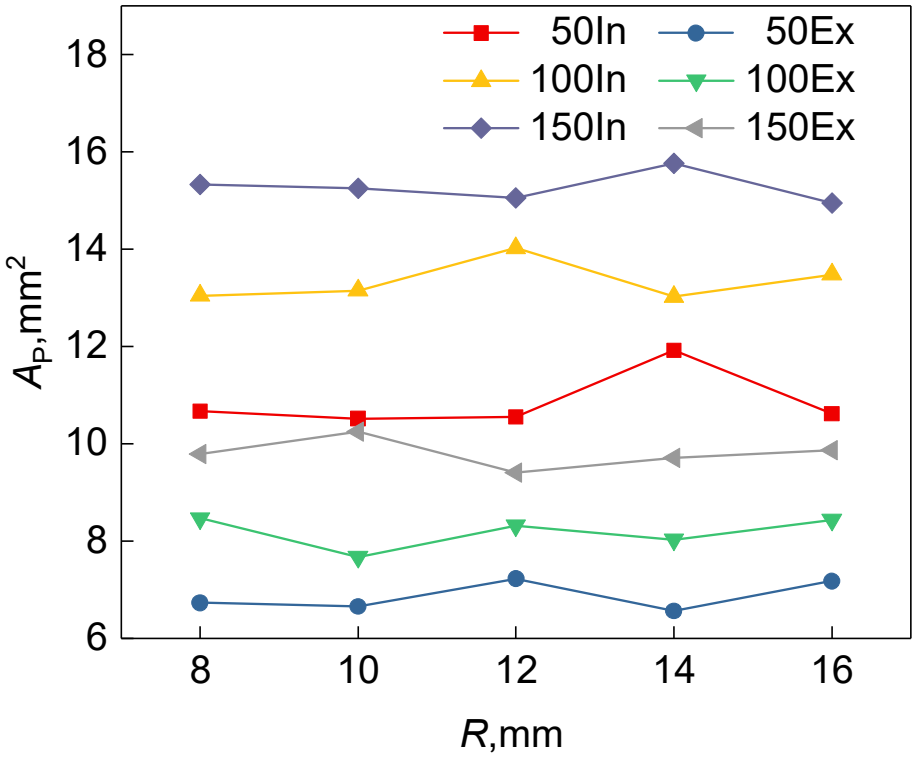

Figure 9. Change Trend of Plastic Zone Area of Different Curvature Radii of Internal Corner and External Corner.

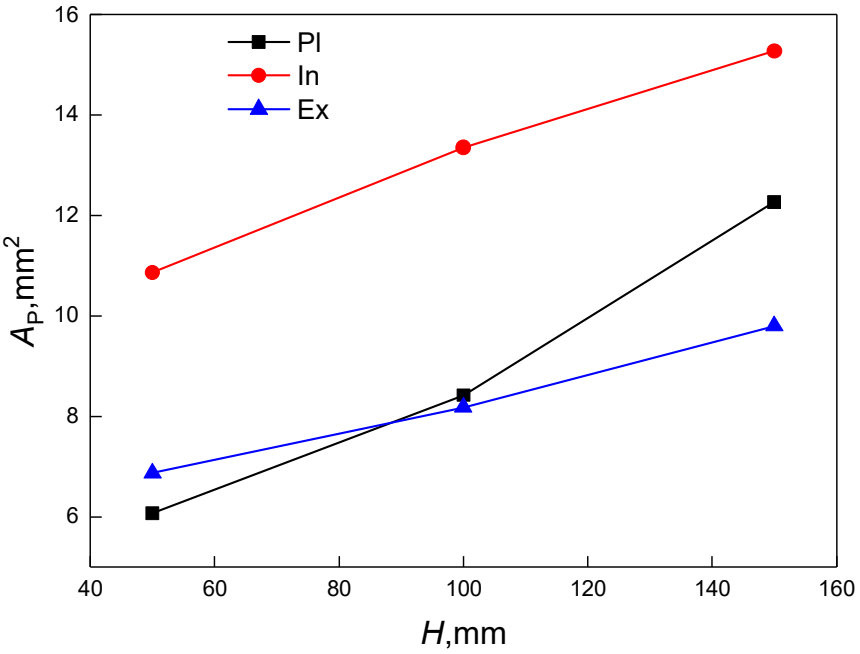

Figure 10. Change Trend of Plastic Zone Area of Plane, Internal Corner and External Corner under Different Impact Strokes.

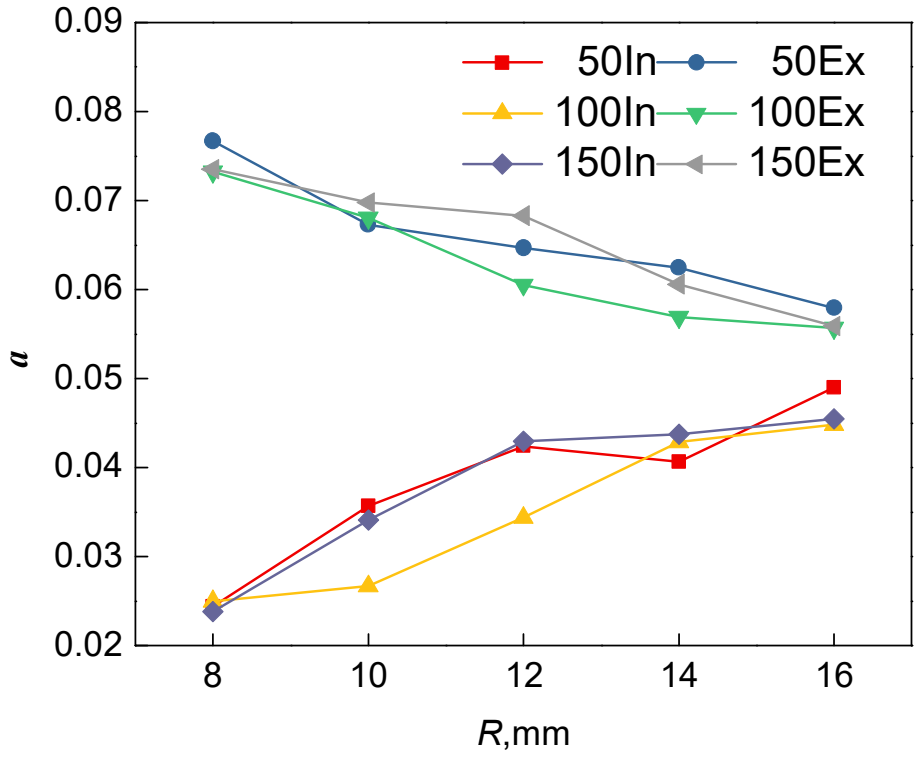

Figure 11. The Change Trend of Deformation Degrees of Internal Corner and External Corner under Different Impact Strokes.

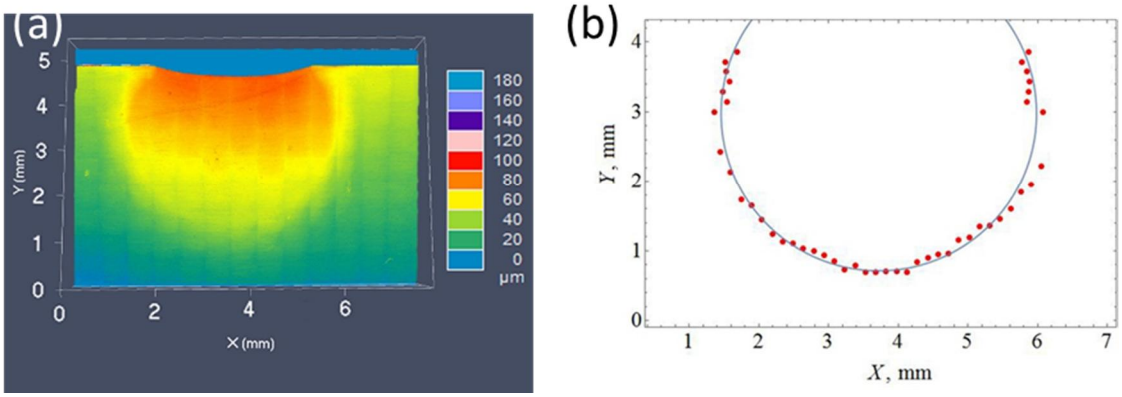

Figure 12. Rebounded Convex Region (a) and Fitting Results of the Effective Boundary Points (b) of Plane.

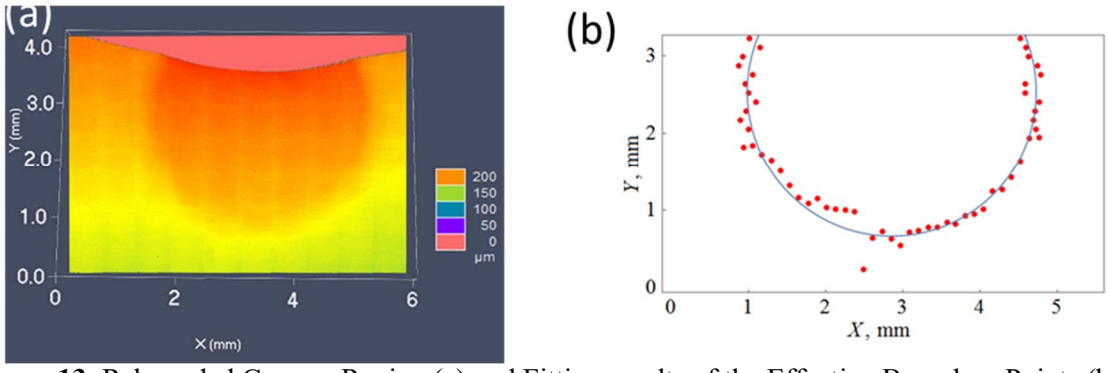

Figure 13. Rebounded Convex Region (a) and Fitting results of the Effective Boundary Points (b) of Curvature 10 mm of External Corner.

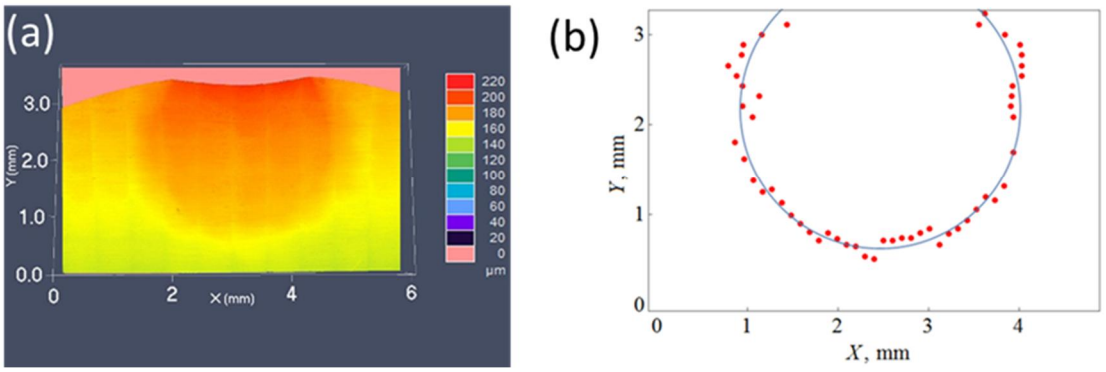

Figure 14. Rebounded Convex Region (a) and Fitting results of the Effective Boundary Points (b) of Curvature 12 mm of External Corner.

4. Conclusions

(1) The hammering method was used to study plastic deformation zone inside the Q235. Mathematical fitting method was used to calculate effective boundary points of each rebound plastic zone. The plastic zones which appeared at internal (In) and external (Ex) curved-surface corners and that appeared at plane-surfaces (Pl) were both circular-shaped, and the spaces around the hammered points were spherical-shaped.

(2) The maximum depth of the hammering plastic zone is 3.92 mm which means that there is still a certain depth of pre-stressed layer after the parts are final processed.

(3) The plastic areas were enlarged with the increase of impact stroke, and those at internal corner surpassed those at external corner with the same impact stroke. As the curvature radius rises, the plastic zone areas did not change significantly. Those plastic areas formed on the plane were changed more quickly than those at the internal external corners.

References

[1] Xiao X D 2015 *Modelling of shot peening stresses and simulation integral deformation of strip peening forming.* Xi'an: Northwest Polytechnical University.
[2] Ma X, Yuan Z T and Liu Y H 2017 *Light Ind. Sci. Technol.* **10** 55.
[3] Zhou Y Q, Zhao Y and Wang P 2010 *Mech. Manag. Dev.* **25(5)** 104.
[4] Hou X Z and Chen L 2017 *Technol. Appl.* **20** 102.
[5] Zou J L 2001 *Die Mould Ind.* **5** 44.
[6] Dong H B and Kang Y L 2011 *Trans. Mater. Heat Treat.* **32(3)** 103.
[7] Chen H N and Tang Y D 1993 *J. Mech. Strength.* **15(3)** 21.
[8] Meng X L 2007 *Numerical simulation of indentation-strain method under different residual stress fields.* Shenyang: Institute of Metal Research Chinese Academy of Sciences.

[9] Jin P and Li X D 2017 *J. Exp. Mech.* **32(5)** 645.
[10] Gai X Y 1993 *Study on yield behaviors of metal surface*. Shenyang: Institute of Metal Research Chinese Academy of Sciences.
[11] Chen H N, Lin Q H, Chen J et al 2001 *Study of plastic zone in residual stress measurement by impact indentation method*. Proc. 10th Nati. Welding Acad. Conf. Harbin: Heilongjiang People's Publishing House 230.
[12] Zhao Z, Chen J, Tan H, Lin X and Huang W D 2017 *Opt. Laser Technol.* **92** 36.
[13] Wang H M, Li R J and Zhou M 2017 *J. Eur. Ceram. Soc.* **37** 2705.
[14] Gu X, Qin J P and Zhang W C 2011 *Chi. Heavy Equip.* **3** 41.
[15] Underwood J H 1973 *Exp. Mech.* **9(1)** 373.
[16] Yu Z F, Zhao Y H, Chen H N et al 2001 *J. Shenyang Arch. Civ. Eng. Univ.* **17(3)** 200.
[17] Chen H N, Lin Q H, Li T R et al 2006 *Trans. Chin. Weld. Inst.* **27(8)** 27.
[18] Chen H N, Lin Q H and Qu P C 2005 *Several basic problems in measuring welding stress by indentation method*. Proc. 11th Nati. Welding Acad. Conf. Harbin: Heilongjiang People's Publishing House 116.
[19] Chen H N, Hu K X and Wu C Z 2010 *Chin. Meas. Teat.* **36(1)** 24.
[20] Maximov J T, Duncheva G V and Ganev N 2012 *J. Construct. Steel Res.* **74** 37.
[21] Hong N 1994 *J. Biomath.* **9(3)** 148.
[22] Cui D Q 2005 *J. Appl. Stat. Manag.* **24(1)** 112.
[23] Xu G W and Liao M C 2002 *J. Wuhan Polytech. Univ.* **4** 104.
[24] Fan L, Liu J H and Wang J L 2016 *J. N.W.T. For. Univ.* **31(3)** 215.
[25] Gao Y K 2004 *Chi. J. Nonferr. Met.* **14(1)** 60.